

Viscous Effects on Elliptic Flow and Shock Waves

I. Bouras¹, L. Cheng^{1,2}, A. El¹, O. Fochler¹, J. Uphoff¹, Z. Xu¹ and C. Greiner¹

¹ Goethe-Universität Frankfurt, Germany

² Huazhong Normal University, Wuhan, China

November 2, 2018

Abstract

Fast thermalization and a strong buildup of elliptic flow of QCD matter as found at RHIC are understood as the consequence of perturbative QCD (pQCD) interactions within the 3+1 dimensional parton cascade BAMPS. The main contributions stem from pQCD bremsstrahlung $2 \leftrightarrow 3$ processes. By comparing to Au+Au data of the flow parameter v_2 as a function of participation number the shear viscosity to entropy ratio is dynamically extracted, which lies in the range of 0.08 and 0.2, depending on the chosen coupling constant and freeze out condition. Furthermore, first simulations on the temporal propagation of dissipative shock waves are given. The cascade can either simulate true ideal shocks as well as initially diluted, truly viscous shocks, depending on the employed cross sections or mean free path, respectively.

1 Introduction: QCD Plasma Thermalization within a pQCD Parton Cascade

The values of the elliptic flow parameter v_2 measured by the experiments at the Relativistic Heavy Ion Collider (RHIC) [1] are (nearly) as large as those obtained from calculations employing ideal hydrodynamics. This finding suggests that a fast local equilibration of quarks and gluons occurs at a very short time scale ≤ 1 fm/c, and that the locally thermalized state of matter created, the quark gluon plasma (QGP), behaves as a nearly perfect fluid. Quarks and gluons should be rather strongly coupled, pointing towards a small viscosity to entropy coefficient for the QGP, which can not be understood by binary pQCD collisions, because they are too weak. This has raised the speculation about nonperturbative interactions as well as about super symmetric representations of Yang-Mills theories using the AdS/CFT conjecture. However, in this talk, we demonstrate that the perturbative QCD (pQCD) can still explain a fast thermalization of the initially nonthermal gluon system, the large collective effects of QGP created at RHIC and the smallness of the shear viscosity to entropy ratio in a consistent manner by using a relativistic pQCD-based on-shell parton cascade Boltzmann approach of multiparton scatterings (BAMPS) [2, 3, 4, 5, 6, 7].

BAMPS is a parton cascade, which solves the Boltzmann transport equation and can be applied to study, on a semi-classical level, the dynamics of gluon matter produced in heavy ion collisions at RHIC energies. The structure of BAMPS is based on the stochastic interpretation of the transition rate [2], which ensures full detailed balance for multiple scatterings. BAMPS subdivides space into small cell units where the operations for transitions are performed. Gluon interactions included in BAMPS are elastic and screened Rutherford-like pQCD $gg \rightarrow gg$ scatterings as well as pQCD inspired

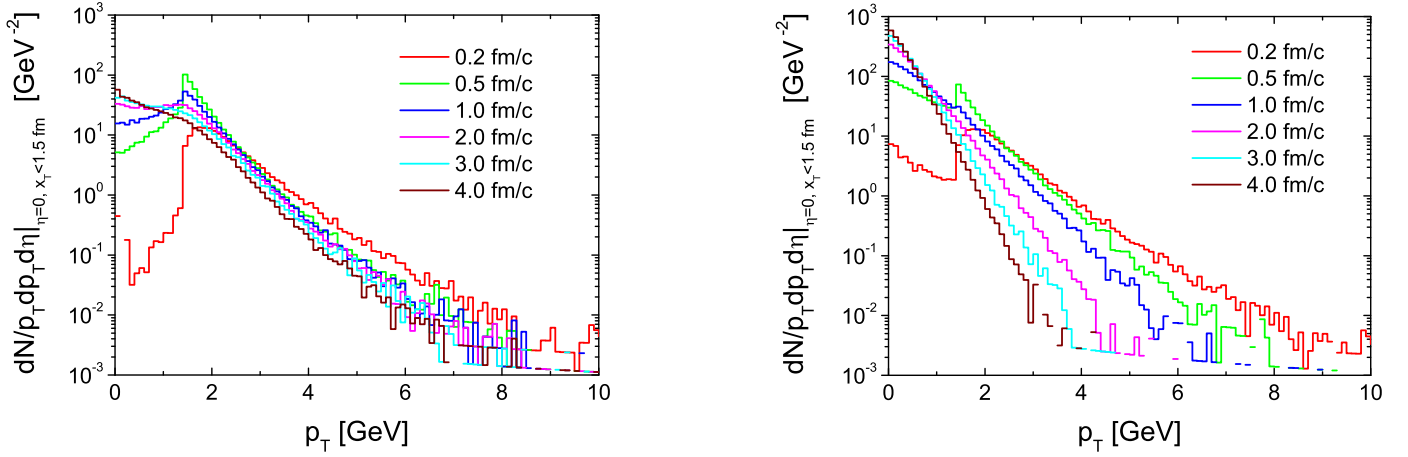


Figure 1: (Color online) Transverse momentum spectrum in the central region at different times obtained from the BAMPs simulation with $gg \rightarrow gg$ only (left panel) and including $gg \leftrightarrow ggg$ collisions (right panel).

bremsstrahlung $gg \leftrightarrow ggg$ of Gunion-Bertsch type. The matrix elements are discussed in the literature [2, 3, 8]. The suppression of the bremsstrahlung due to the Landau-Pomeranchuk-Migdal (LPM) effect is taken into account within the Bethe-Heitler regime employing a step function in the infrared regime, allowing for independent gluon emissions.

In the default simulations, the initial gluon distributions are taken in a Glauber geometry as an ensemble of minijets with transverse momenta greater than 1.4 GeV [3], produced via semihard nucleon-nucleon collisions. The later interactions of the gluons are terminated when the local energy density drops below 1 GeV/fm³ [3, 6] to 0.6 GeV/fm³ [7]. The minijet initial conditions and the subsequent evolution using the present prescription of BAMPs for two sets of the coupling $\alpha_s = 0.3$ and 0.6 give nice agreements to the measured transverse energy per rapidity over all rapidities [6, 7].

As a first example the fast thermalization of gluons is demonstrated in a local and central region which is taken as an expanding cylinder with a radius of 1.5 fm and within an interval of space time rapidity $-0.2 < \eta < 0.2$. Figure 1 shows the varying transverse momentum spectrum with time obtained from the BAMPs calculations for central Au+Au collisions at $\sqrt{s} = 200A$ GeV, with elastic pQCD $gg \rightarrow gg$ only (left panel) and including pQCD-inspired bremsstrahlung $gg \leftrightarrow ggg$ (right panel), respectively ($\alpha_s = 0.3$ is used). One clearly sees that not much happens in the left panel of figure 1. With only elastic pQCD interactions the gluon system is initially nonthermal and also stays in a nonthermal state at late times. The situation is dramatically changed when the inelastic interactions are included. In the right panel of figure 1 we see that the spectrum reaches an exponential shape at 1 fm/c and becomes increasingly steeper at late times. This is a clear indication for the achievement of local thermal equilibrium and the onset of hydrodynamical collective expansion with subsequent cooling by longitudinal work.

The inelastic pQCD based bremsstrahlung and its back reaction are essential for the achievement of local thermal equilibrium at a short time scale. The fast thermalization happens in a similar way if color glass condensate is chosen as the initial conditions. One of the important messages obtained there is that the hard gluons thermalize at the same time as the soft ones due to the $ggg \rightarrow gg$ process, which is not included in the so called standard “Bottom Up” scenario of thermalization [4]. The situation is also the same when employing PYTHIA based initial conditions [9].

2 Shear Viscosity and Elliptic Flow

Kinetic equilibration relates to momentum deflection. Large momentum deflections due to large-angle scatterings will speed up kinetic equilibration. Whereas the elastic pQCD scatterings favor small-angle collisions, the collision and emission angles in bremsstrahlung processes are, for lower invariant, i.e. thermal energies, rather isotropically distributed due to the incorporation of the LPM cutoff [2, 3]. Hence, although the elastic cross section is still considerably larger than the inelastic one, the given argument is the intuitive reason why the bremsstrahlung processes are acting more effectively in the equilibration of the gluon matter than the elastic interactions. Quantitatively it was shown in detail in [3] that the contributions of the different processes to momentum isotropization are quantified by the so called transport rates

$$R_i^{\text{tr}} = \frac{\int \frac{d^3p}{(2\pi)^3} \frac{p_z^2}{E^2} C_i[f] - \langle \frac{p_z^2}{E^2} \rangle \int \frac{d^3p}{(2\pi)^3} C_i[f]}{n \left(\frac{1}{3} - \langle \frac{p_z^2}{E^2} \rangle \right)},$$

where $C_i[f]$ is the corresponding collision term describing various interactions, $i = gg \rightarrow gg, gg \rightarrow ggg, ggg \rightarrow gg$, respectively. The sum of them gives exactly the inverse of the time scale of momentum isotropization, which also marks the time scale of overall thermalization. It turns out that $R_{gg \rightarrow ggg}^{\text{tr}}$ is a factor of 3 – 5 larger than $R_{gg \rightarrow gg}^{\text{tr}}$ over a wide range in the coupling constant, which demonstrates the essential role of the bremsstrahlung in thermal equilibration [3].

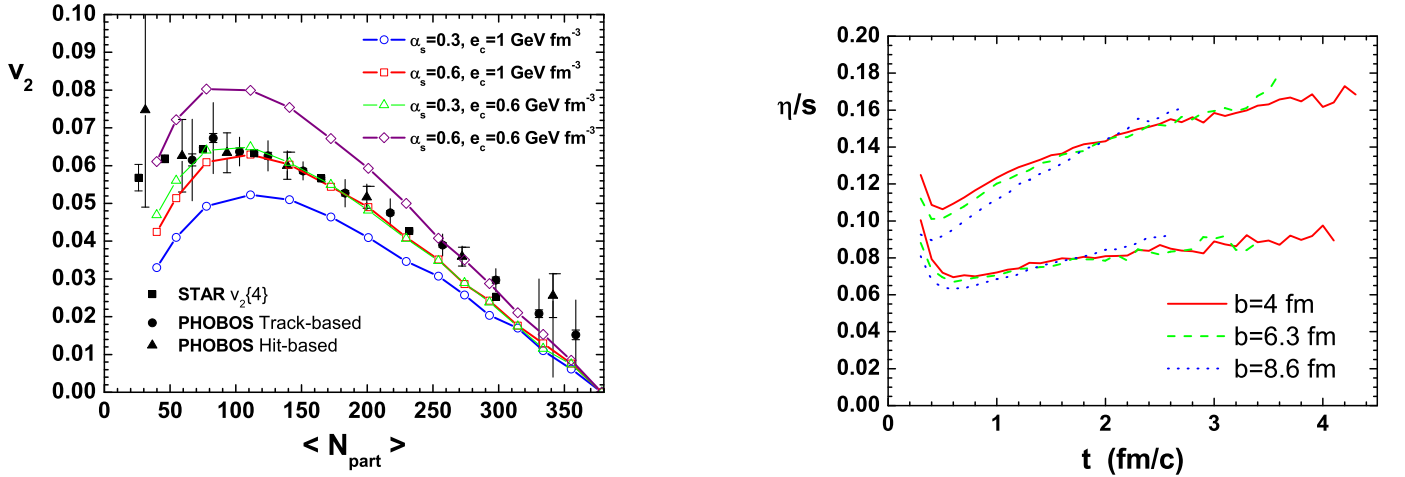


Figure 2: (color online) Left panel: Elliptic flow vs. N_{part} for Au+Au collisions at $\sqrt{s_{NN}} = 200$ GeV. The points are STAR [13] and PHOBOS [12] data for charged hadrons within $|\eta| < 0.5$ and $|\eta| < 1$, respectively, whereas the curves with symbols are results for gluons within $|\eta| < 1$, obtained from the BAMPS calculations with $\alpha_s = 0.3$ and 0.6 and with two freezeout energy densities, $e_c = 0.6$ and 1 GeV fm^{-3} . Right panel: the shear viscosity to entropy density ratio η/s at the central region during the entire expansion. η/s values are extracted from the simulations at impact parameter $b = 4, 6.3$, and 8.6 fm. The upper band shows the results with $\alpha_s = 0.3$ and the lower band the results with $\alpha_s = 0.6$.

Employing the Navier-Stokes approximation the shear viscosity η is directly related to the transport rate [5],

$$\eta \cong \frac{1}{5} n \frac{\langle E(\frac{1}{3} - \frac{p_z^2}{E^2}) \rangle}{\frac{1}{3} - \langle \frac{p_z^2}{E^2} \rangle} \frac{1}{\sum R^{\text{tr}} + \frac{3}{4} \partial_t(\ln \lambda)},$$

where λ denotes the gluon fugacity. This expression allows to calculate the viscosity dynamically and locally in a full and microscopical simulation (see Figure 2). On the other hand, close to thermal equilibrium the expression reduces to the more intuitive form $\eta = \frac{4}{15} \sum \frac{\epsilon}{R^{\text{tr}}}$ and thus for the shear viscosity to

entropy ratio $\frac{\eta}{s} = \left(5\beta R_{gg \rightarrow gg}^{\text{tr}} + \frac{25}{3}\beta R_{gg \rightarrow ggg}^{\text{tr}}\right)^{-1}$. Within the present description bremsstrahlung and its back reaction lower the shear viscosity to entropy density ratio significantly by a factor of 7, compared with the ratio when only elastic collisions are considered. For $\alpha_s = 0.3$ one finds $\eta/s = 0.13$ [5, 4]. To match the lower bound of $\eta/s = 1/4\pi$ from the AdS/CFT conjecture $\alpha_s = 0.6$ has to be employed. Even for that case the cross sections are in the order of 1 mb for a temperature of 400 MeV. The numbers for the viscosity slightly increase up to 20 percent when calculating it by means of Grads momentum method and using the 2nd order Israel-Stewart framework of dissipative relativistic hydrodynamics [10]. In any case, perturbative QCD interactions can drive the gluon matter to a strongly coupled system with an η/s ratio as small as the lower bound from the AdS/CFT conjecture.

The elliptic flow $v_2 = \langle (p_x^2 - p_y^2)/p_T^2 \rangle$ can be directly calculated from microscopic simulations for Au+Au collisions at $\sqrt{s} = 200$ A GeV employing BAMPS. $\alpha_s = 0.3$ and 0.6 and also two values of the critical energy density e_c for the freezeout are used for comparisons [6, 7]. For a firm footing we compare our results with the experimental data, assuming parton-hadron duality. The left panel of Figure 2 shows the elliptic flow v_2 at midrapidity for various centralities (impact parameters), compared with the PHOBOS [12] and STAR [13] data. Except for the central centrality region the results with $\alpha_s = 0.6$ agree perfectly with the experimental data, whereas the results with $\alpha_s = 0.3$ are roughly 20% smaller. On the other hand, one also sees that the v_2 results with $\alpha_s = 0.3$ and $e_c = 0.6 \text{ GeVfm}^{-3}$ (green curves with open triangles) are almost identical with those with $\alpha_s = 0.6$ and $e_c = 1 \text{ GeVfm}^{-3}$ (red curves with open squares). Stronger interactions or longer QGP phase leads to the same final values of v_2 . Hence, according to the present study, η/s is most probably lying between 0.2 and 0.08. These findings are in line with a similar study of the Catania group employing a parton cascade with binary and isotropic interactions and large cross sections [11]. In the present case, however, the generation of the large elliptic flow observed at RHIC is well described by pure perturbative gluon interactions as incorporated in BAMPS.

We note that adding quark degrees of freedom into the dynamical evolution of the QCD matter with a detailed understanding of the hadronization of gluons and quarks and the late stage hadronic interactions will further be helpful in explaining the viscous facets of the final hadron elliptic flow (for a discussion see [7]). Also different picture of initial condition (eg. color glass condensate) may also lead to different initially spatial eccentricity, and, hence, will moderately affect the final value of v_2 . These investigations are underway and will provide more constrains on extracting η/s .

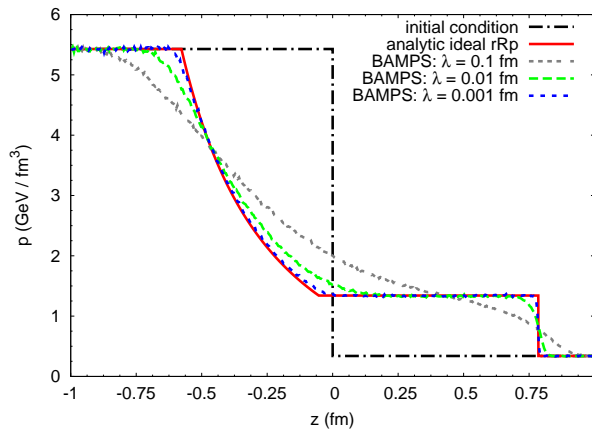


Figure 3: (Color online) Pressure profile at time $t = 1 \text{ fm/c}$ of a longitudinal shock developing from an initial Riemann singularity with $T_{\text{left}} = 400 \text{ MeV}$ and $T_{\text{right}} = 200 \text{ MeV}$ for various finite, but increasingly small mean free path of the colliding partons. For comparison, the analytical solution of the Riemann problem for ideal relativistic hydrodynamics is also depicted by the red solid curve.

3 Dissipative Relativistic Shock Waves

The quenching of gluonic jets can also be self-consistently addressed within the same full simulation of BAMPS [8] including elastic and radiative collisions. The nuclear modification factor R_{AA} of gluons is obtained directly by taking the ratio of the final p_T spectra to the initial mini-jet spectra. A clear suppression of high- p_T gluon jets at a roughly constant level of $R_{AA}^{\text{gluons}} \approx 0.06$ is found. The dominant contribution for the energy loss is the bremsstrahlung [8]. The suppression is approximately a factor of three stronger than the experimental pion data. However, at present, the simulation does not include any light quarks, which are expected to lose less energy by a significant factor of 4/9 compared with gluons. A more detailed microscopic understanding of the various phenomena related to high energy jets in the parton matter represents an intriguing, ongoing project.

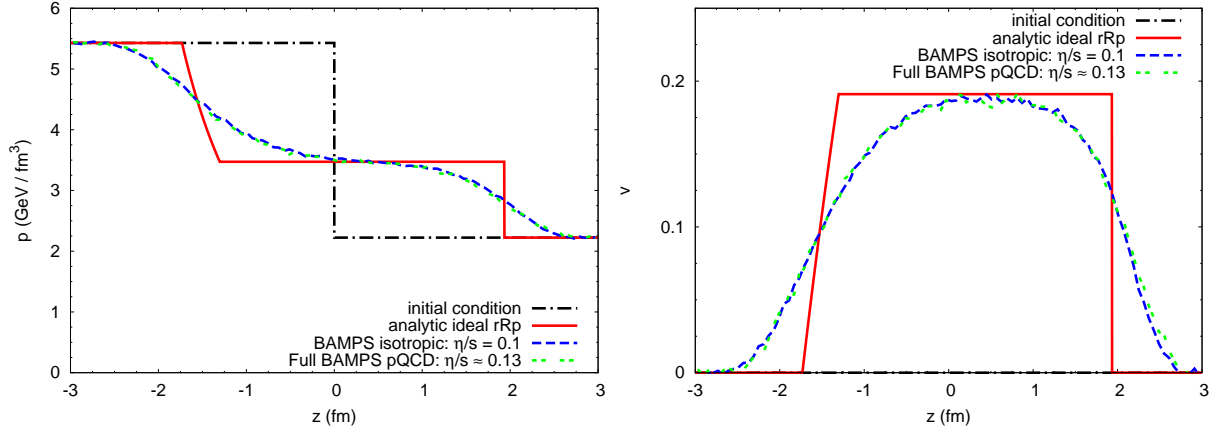


Figure 4: (Color online) Pressure profile (left panel) and velocity profile (right panel) at time $t = 3\text{fm}/c$ of a longitudinal shock developing from an initial Riemann singularity with $T_{\text{left}} = 400$ MeV and $T_{\text{right}} = 320$ MeV for a plasma with a fixed shear viscosity to entropy ratio of 0.1 (with binary and isotropic scattering) and for a plasma with the full pQCD BAMBS simulation ($\alpha_s = 0.3$) including bremsstrahlung processes. The analytical solution of the Riemann problem for ideal relativistic hydrodynamics is also depicted by the red solid curve.

Experimentally a significant and exciting structure in the two-particle and three-particle correlations of associated particles of a high energy jet has been observed, which might be the result of the conical emission of propagating Mach cones created by a jet crossing the expanding medium [14]. Nuclear shock waves have been proposed since a long time in the context of heavy ion collisions. Recent calculations invoking ideal hydrodynamics for the QCD matter support a picture of creation of Mach cones associated with a jet losing significant energy [15]. At present it is yet not possible to see developing Mach cone-like structures within the cascade BAMPS, as jet-quenching has to be further understood and such simulations (will) need intensive computing time.

An important question to be answered aside is whether relativistic shock waves can be observed in parton cascade simulations and how finite (shear) viscosity will alter such a picture. In the following we report on a very recent study [16].

A particular case of a to be created shock wave represents the well established (relativistic) Riemann problem: At a particular layer (eg the x-y-plane) there is an initial discontinuity in pressure and energy density of thermalized matter. Within an ideal hydrodynamic framework the further temporal evolution can be solved (semi-)analytically for a given equation of state. Typically an immediate shock wave evolves to the side of lower density whereas a rarefaction wave evolves to the side of higher density.

To make the computing time consumption tolerable, for most of the calculations only $2 \leftrightarrow 2$ collisions

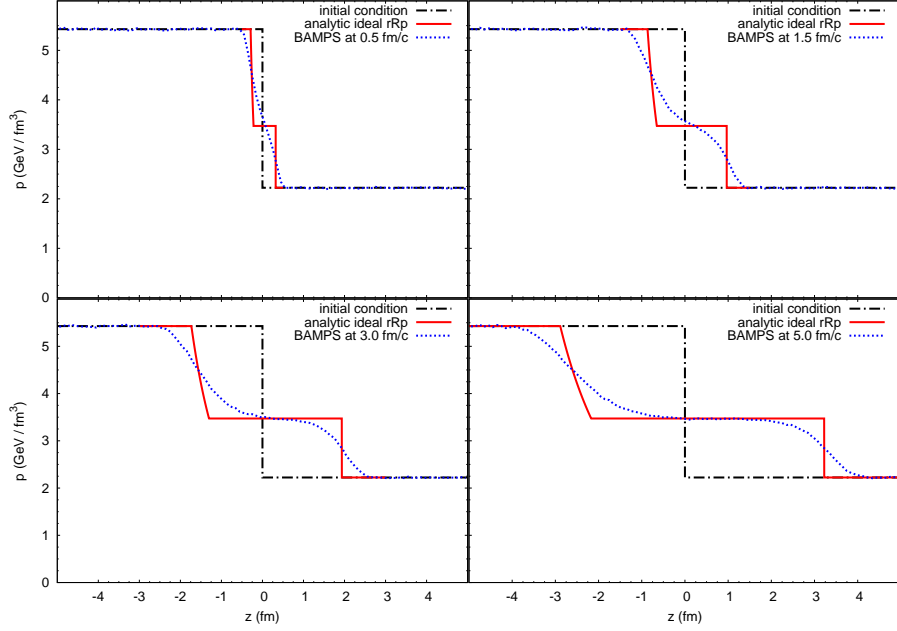


Figure 5: (Color online) Pressure profile at various times ($t = 0.5, 1.5, 3, 5$ fm/c) of a longitudinal shock (with $T_{\text{left}} = 400$ MeV and $T_{\text{right}} = 320$ MeV) for a plasma with fixed shear viscosity to entropy ratio of $\frac{\eta}{s} = \frac{1}{4\pi}$ referring to the lower bound of the AdS/CFT conjecture.

with a isotropic cross section are employed. Either a constant mean free path in the computational frame via

$$\lambda_{\text{mfp}} = \frac{\gamma(z, t)}{n(z, t) \sigma(z, t)}$$

or a constant shear viscosity to entropy ratio via

$$\frac{\eta}{s} = \frac{16}{45} \frac{\epsilon(z, t)}{n(z, t) \sigma(z, t)} \frac{1}{4n(z, t) - n(z, t) \ln(\lambda(z, t))}$$

can be employed, where n counts the local gluon density, σ the local cross section, $\gamma = 1/\sqrt{1 - v^2}$ the Lorentz factor, ϵ the local energy density, and λ the local gluon fugacity.

In Figure 3 calculations of a particular example of the Riemann problem are shown, when a (variety of fixed) mean free path (for isotropic binary collisions) is chosen. Details of the simulations are in ref. [16]. Shown is the pressure profile at a time $t = 1$ fm/c of a longitudinal shock developing from an initial Riemann singularity at $z = 0$ fm with $T_{\text{left}} = 400$ MeV and $T_{\text{right}} = 200$ MeV. The mean free paths of the colliding partons are increasingly small. The matter would have an unrealistic small shear viscosity to entropy ratio η/s of about 0.04, 0.004, 0.0004. For comparison, the analytical solution of the Riemann problem for ideal relativistic hydrodynamics is depicted by the red solid curve. One nicely recognizes how the correct limit of ideal hydrodynamics is achieved, which is nontrivial! Only for tiny shear viscosities the shock waves do resemble that of the ideal case. The present calculations do present a cornerstone for investigating dissipative shock waves within transport simulations.

Figure 4 shows the pressure profile (left panel) and velocity profile (right panel) at a time $t = 3$ fm/c of a longitudinal shock developing from an initial Riemann singularity at $z = 0$ fm with $T_{\text{left}} = 400$ MeV and $T_{\text{right}} = 320$ MeV for a plasma with a fixed shear viscosity to entropy ratio of 0.1 (with binary and isotropic scattering) and for a gluon plasma with the *full* pQCD BAMBS simulation ($\alpha_s = 0.3$) including

bremsstrahlung processes. Both calculations basically agree as η/s in the full simulation is about 0.13. Hence the full pQCD simulations would give rather dissipative shock waves. Yet such calculations are, in principle, though extremely time consuming, possible. It remains to be seen whether Mach cone like structures can be built up and maintained in realistic 3+1 dimensional calculation when a jet is produced and loses energy to the medium. This remains a formidable task for the future.

In Figure 5 the temporal evolution of the pressure profile of a longitudinal shock (with $T_{\text{left}} = 400$ MeV and $T_{\text{right}} = 320$ MeV) for a plasma with fixed shear viscosity to entropy ratio of the celebrated AdS/CFT conjectured value of $\frac{\eta}{s} = \frac{1}{4\pi}$ is shown. For small times $t \leq 2$ fm/c the situation rather looks like a diffusion process [16] and one might not really speak about a (fully) developed shock wave. On the other hand, for longer times the characteristic shock plateau develops and the overall situation resembles that of an ideal shock with selfsimilar properties. A special Knudsen number may characterize whether a shock has developed or not [16].

In summary, dissipative shocks can be nicely simulated and investigated with parton cascade BAMPS. Whether Mach cone-like behaviour can be observed within realistic simulations for RHIC is an exciting issue, as the QGP life time is not long and the medium is indeed viscous. In addition, cascade simulations provide an excellent basis for testing numerical algorithms for the various developing dissipative hydrodynamical theories.

Acknowledgments: We are grateful to the Center for the Scientific Computing (CSC) at Frankfurt for the computing resources. This work was supported by BMBF, DAAD, DFG, GSI and by the Helmholtz International Center for FAIR within the framework of the LOEWE program (Landes-Offensive zur Entwicklung Wissenschaftlich-ökonomischer Exzellenz) launched by the State of Hesse.

References

- [1] S. Adler et al. (PHENIX Collaboration), Phys. Rev. Lett. **91** 182301 (2003);
J. Adams et al. (STAR Collaboration), Phys. Rev. Lett. **92** 052302 (2004).
- [2] Z. Xu and C. Greiner, Phys. Rev. C **71** 064901 (2005).
- [3] Z. Xu and C. Greiner, Phys. Rev. C **76** 024911 (2007).
- [4] A. El, Z. Xu, and C. Greiner, Nucl. Phys. A **806**, 287 (2008).
- [5] Z. Xu and C. Greiner, Phys. Rev. Lett. **100**, 172301 (2008).
- [6] Z. Xu, C. Greiner, and H. Stöcker, Phys. Rev. Lett. **101**, 082302 (2008).
- [7] Z. Xu and C. Greiner, arXiv:0811.2940 [hep-ph].
- [8] O. Fochler, Z. Xu, and C. Greiner, arXiv:0806.1169 [hep-ph].
- [9] L. Cheng et al, in preparation.
- [10] A. El et al, in preparation.
- [11] G. Ferini, M. Colonna, M. Di Toro, and V. Greco, e-Print: arXiv:0805.4814[nucl-th];
see also contribution by V. Greco in these proceedings.
- [12] B. Back et al. (PHOBOS Collaboration), Phys. Rev. C **72** 051901(R) (2005).
- [13] J. Adams et al. (STAR Collaboration), Phys. Rev. C **72** 014904 (2005).
- [14] J. G. Ulery (STAR Collaboration), Int. J. Mod. Phys. E **16**, 2005 (2007).
- [15] B. Betz, M. Gyulassy, D. H. Rischke, H. Stocker and G. Torrieri, J. Phys. G **35**, 104106 (2008).
- [16] I. Bouras, ‘Stosswellenphänomene in einer partonischen Kaskade’, master thesis 2008;
manuscript in preparation.